

# Delivery and Quantification of Hydrogen Peroxide Generated via Cold Atmospheric Pressure Plasma through Biological Material

H. J. Hathaway<sup>1\*</sup>, B. L. Patenall<sup>2</sup>, N. T. Thet<sup>2</sup>, A. C. Sedgwick<sup>2</sup>, G. T. Williams<sup>2</sup>, A. T. A. Jenkins<sup>2</sup>, S. L. Allinson<sup>3</sup> and R. D. Short<sup>1</sup>

<sup>1</sup> Department of Chemistry, Lancaster University, Lancaster, UK

<sup>2</sup> Department of Chemistry, University of Bath, Bath, UK

<sup>3</sup> Division of Biomedical and Life Sciences, Lancaster University, Lancaster, UK

\*E-mail: [holliejanehathaway@gmail.com](mailto:holliejanehathaway@gmail.com)

Received xxxxxx

Accepted for publication xxxxxx

Published xxxxxx

## Abstract

The ability of plasma-generated hydrogen peroxide ( $H_2O_2$ ) to traverse bacterial biofilms and the subsequent fate of the generated  $H_2O_2$  has been investigated. An *in vitro* model, comprising a nanoporous membrane impregnated with artificial wound fluid and biofilms of varying maturity was treated with a helium-driven, cold atmospheric pressure plasma jet. The concentration of  $H_2O_2$  generated below the biofilms was quantified. The results showed that the plasma-generated  $H_2O_2$  interacted significantly with the biofilm, thus exhibiting a reduction in concentration across the underlying nanoporous membrane. Biofilm maturity exhibited a significant effect on the penetration depth of  $H_2O_2$ , suggesting that well established, multilayer biofilms are likely to offer a shielding effect with respect to cells located in the lower layers of the biofilm, thus rendering them less susceptible to plasma disinfection. This may prove clinically significant in the plasma treatment of chronic, deep tissue infections such as diabetic and venous leg ulcers. Our results are discussed in the context of plasma-biofilm interactions, with respect to the fate of the longer lived reactive species generated by cold atmospheric pressure plasma, such as  $H_2O_2$ .

Keywords: cold atmospheric pressure plasma, hydrogen peroxide, bacterial biofilm

## 1. Introduction

The ability to treat antibiotic resistant microorganisms has become paramount in the fight against bacterial infection owing to their ever-increasing prevalence. The apparent stagnation in antimicrobial drug development has fuelled urgent initiatives from a number of prominent healthcare organisations tailored towards treating and ultimately preventing such infections [1-3]. The extent of the current crisis is exemplified according to a predicted annual death toll of 10 million by 2050 arising solely from drug resistant

infections (surpassing that of cancer) [4]. In addition to antimicrobial resistance (both *de novo* and pre-existing), the ability of bacteria to form biofilms, (dense, multilayer communities of bacterial cells protected by an extracellular polymeric substance (EPS)), further encumbers effective disinfection owing to changes in the physiological state of the cells contained within. Notoriously difficult to treat, it is estimated that biofilms are associated with 65% of all bacterial infections, rising to 85% when considering chronic infections [5]. Biofilms are able to form on a multitude of surfaces; both biotic and abiotic, thus providing a significant reservoir of

1  
2  
3 pathogenic microorganisms responsible for numerous human  
4 infections. Biofilms are reported to be involved in half of all  
5 hospital-acquired infections, which the World Health  
6 Organisation estimates to affect 4.5 million people per annum  
7 in Europe, highlighting the significant challenge currently  
8 facing the global healthcare community [6, 7].  
9

10 Wound infections, specifically chronic wound infections have  
11 a reported prevalence of 6% in the UK and account for at least  
12 5.5% of the total NHS expenditure [8]. In the USA such non-  
13 healing wounds carry an annual cost of \$25 billion and it has  
14 been estimated that 1-2% of the population in developed  
15 countries will develop a chronic wound in their lifetime [9].  
16 Wounds (venous, pressure, arterial and diabetic) are the  
17 leading cause of amputation, the latter being responsible for  
18 70% of all lower limb amputations which occur globally every  
19 30 seconds as a direct result of non-healing diabetic ulcers [10,  
20 11]. The protective nature of the EPS along with the induction  
21 of various quorum sensing pathways and the subsequent  
22 alteration in gene expression, has rendered biofilms largely  
23 recalcitrant to common antimicrobial agents. Hence, the need  
24 for effective treatment strategies has become imperative in  
25 reducing both the social and economic burden of wound  
26 infection [12].  
27

28 Cold atmospheric pressure plasma (CAP) has been proven to  
29 deliver a potent antimicrobial cocktail of reactive species able  
30 to successfully decontaminate numerous clinically relevant  
31 single- and mixed-species biofilms, including those associated  
32 with significant drug resistance; termed the 'ESKAPE'  
33 pathogens [13-15]. The composition and delivery of reactive  
34 species generated during CAP therapy, such as reactive  
35 oxygen and nitrogen species (RONS) may be controlled  
36 according to the plasma parameters employed, providing an  
37 attractive therapeutic treatment option currently undergoing  
38 significant investigation within the scientific community [16,  
39 17]. Extensive discussion can be found in the literature  
40 surrounding the effects of the plasma source, the variation in  
41 operating conditions and the current progress and challenges  
42 facing CAP therapy in the control of microbial biofilms and  
43 wound infection [18-22]. The interaction of non-thermal  
44 plasma with biological material has been well documented in  
45 terms of bactericidal effects, phenotypic and genetic  
46 consequences (in both eukaryotic and prokaryotic cells) and  
47 with respect to plasma-activated liquids [23-25]. Studies have  
48 been conducted using tissue surrogates such as gelatin and  
49 agarose, alongside cellular mimics such as phospholipid  
50 vesicles to track plasma delivery of RONS [26-30].  
51 Furthermore, the biofilm penetration depth of CAP-generated  
52 reactive species has been reported as a function of cell death  
53 and via computational modelling [31-33]. However, the direct  
54 quantification of longer-lived species, such as hydrogen  
55 peroxide ( $H_2O_2$ ) has yet to be conducted through living  
56 biofilms. This study reports the effects of biofilm composition

on the delivery of plasma-generated  $H_2O_2$  across the cellular  
interface, thus confirming the ability of biologically active  
plasma-generated products to traverse bacterial biofilms  
according to biofilm density/maturity. The presence of  $H_2O_2$ ,  
or lack thereof, may provide insight into the fate of the longer-  
lived species generated by CAP and the subsequent  
implications this may have for the safe and effective  
decontamination of chronic wounds.

## 2. Materials and Methods

### 2.1 Materials

Tryptic Soy Broth (TSB), Tryptic Soy Agar (TSA), Luria-  
Bertani (LB) broth, phosphate buffered saline (PBS) tablets  
(pH 7.4), Brain Heart Infusion (BHI) agar, foetal calf serum  
(FCS) (HyClone), sodium chloride (NaCl), potassium iodide  
(KI),  $H_2O_2$ , peptone, poly (vinyl alcohol) (PVA) ( $M_w$  14600–  
18600  $g\ mol^{-1}$ ), carboxymethyl cellulose (CMC) and agarose  
were all purchased from Sigma-Aldrich, UK. Biofilms were  
formed on sterile, nanoporous polycarbonate filter membranes  
(Whatman), 19 mm in diameter with an average pore size of  
200 nm.

### 2.2 CAP jet

The plasma jet used consists of a single electrode  
configuration with a 150 mm glass capillary tube and a 15 mm  
external ring copper electrode operating at a distance of 40  
mm from the end of the tube [30]. Helium was used as the  
carrier gas at a fixed flow rate of 0.6 standard litres per minute  
(SLPM). The jet was operated at an applied voltage of 10 kV  
 $p-p$  and a frequency of 25 kHz. The distance from the end of  
the capillary tube to the surface of the substrate was 5 mm.  
The jet used predominantly produces  $H_2O_2$  under the  
described operation parameters [28]. There is evidence that  
the initial interaction of the plasma with ambient air in the gas  
phase is the primary production site for  $H_2O_2$  [34].

### 2.3 Quantification of $H_2O_2$

Potassium iodide (KI) was used to quantify  $H_2O_2$   
concentration in solution via the generation of a standard  
curve. 1M KI in deionised (DI) water was added to varying  
concentrations of  $H_2O_2$  at a ratio of 1:1 and incubated at 25 °C  
for 30 minutes. Absorbance measurements were taken at 410  
nm using a microplate reader (Spectrostar Omega, BMG  
Labtech) and used to produce a calibration curve  
(Supplementary Information Figure 1) [35]. For quantification  
of plasma-generated  $H_2O_2$  in PBS, 350  $\mu$ L of PBS was added  
to each well in a 96 well microtiter plate and treated for 0.5 -  
5 minutes. 100  $\mu$ L of the treated solution was then removed,  
added to 1M KI (1:1 v/v) and incubated at 25 °C for 30  
minutes. Absorbance measurements were taken as before and  
the concentration calculated using the calibration curve.

## 2.4 Bacterial strains and growth conditions

Methicillin-resistant *Staphylococcus aureus* (MRSA) 252 and *Pseudomonas aeruginosa* (*P. aeruginosa*) PA01 were sourced from a bacterial strain collection belonging to the Biophysical Research Group housed at the University of Bath, UK. Single colonies were cultured from freezer stocks (stored at -80 °C) on TSA or LB agar for MRSA 252 and PA01, respectively. Overnight cultures were grown from single colonies in TSB or LB liquid media for MRSA 252 and PA01, respectively. Cultures were incubated at 37°C with agitation (200 rpm) for 18 hours to achieve a cell density of 10<sup>9</sup> colony forming units (CFU) / ml.

## 2.5 Bacterial biofilm formation

Overnight cultures of MRSA 252 and PA01 were centrifuged at 10,000 x g for 10 minutes, washed and resuspended in fresh PBS to an optical density of ~ 0.2 (~ 10<sup>6</sup> CFU/ml). White sterile polycarbonate filter membranes positioned on BHI agar were inoculated with 20 µL artificial wound fluid (FCS mixed in equal volume with 0.85% NaCl and 0.1% peptone) in order to better model the wound environment and components supporting bacterial growth and adhesion. 30 µL of bacterial subculture was added to the conditioned membranes. Membranes were UV sterilised for 10 minutes prior to bacterial inoculation. Plates were incubated at 32°C for 8, 12 and 24 hours [36].

## 2.6 Quantification of viable bacterial cells

Following incubation, biofilms were removed from the plates and transferred into 5 mL of PBS. The solutions were vortexed at 3000 rpm for 1 minute and sonicated for 15 minutes. This process was repeated twice to ensure complete detachment of the bacterial cells from the membrane. Serial dilutions were carried out in PBS and plated on TSA or LB agar with subsequent incubation at 37°C for 24 hours to enumerate the number of viable bacteria.

## 2.7 CAP treatment of bacterial biofilms

Bacterial biofilms grown for 8, 12 and 24 hours were placed atop 350 µL of PBS in a 96 well microtiter plate (full experimental set-up is shown in Figure 2 Supplementary Information). Biofilms were plasma treated for 5 minutes, with manual movement of the jet around the circumference of the well similarly as *in vivo* wound treatments. Following plasma treatment, 100 µL of PBS was removed from each well and the concentration of H<sub>2</sub>O<sub>2</sub> determined as before via correlation to the standard curve. In order to assess any time-dependent generation of H<sub>2</sub>O<sub>2</sub> as a result of plasma treatment, additional 8 hour biofilms were subject to plasma treatment followed by a further 4 hour incubation *in situ* at 32 °C prior to H<sub>2</sub>O<sub>2</sub> quantification. Separate experiments were undertaken

to quantify the number of viable bacterial cells (post plasma treatment) as previously described. All experiments were conducted in triplicate for each bacterial species and each time point.

## 2.8 Temperature measurement of plasma jet

The temperature of the CAP jet and biofilm onto which the jet was directed was measured using a Xenics® GOBI-640-GigE thermal imaging camera. Plasma temperature was assessed when treating a PA01 biofilm grown for 24 hours and placed atop 350 µL PBS in 96 well microtiter plate.

## 2.9 Topical application of H<sub>2</sub>O<sub>2</sub>

The effect of H<sub>2</sub>O<sub>2</sub> on bacterial survival was investigated via topical application of H<sub>2</sub>O<sub>2</sub> to 8, 12 and 24 hour biofilms of both MRSA 252 and PA01. 100 µL of 550 µM H<sub>2</sub>O<sub>2</sub> (the same concentration of H<sub>2</sub>O<sub>2</sub> produced in solution by the plasma jet in 5 minutes) was applied to the surface of the biofilms. The concentration of H<sub>2</sub>O<sub>2</sub> below the biofilms was quantified after 5 minutes, and after 4 hours incubation at 32 °C as previously described.

## 2.10 Hydrogel formulation

PVA/ CMC hydrogels were prepared by dissolving PVA (5% w/v) in DI water and heating to 97 °C with constant stirring to facilitate dissolution. The solution was supplemented with 0.5% w/v CMC, cast to a thickness of 1 mm and stored for 18 hours at -20 °C to promote cryogenic gelation. Discs of gel were cut to a diameter of ~1 cm before being placed atop 350 µL PBS in a 96 well plate and subject to CAP treatment.

Agarose hydrogels were prepared by dissolving agarose (1.5% w/v) in DI water and heating to 90 °C. The solution was cooled, supplemented with 0.5 M KI and cast to a thickness of 1 cm. Biofilms were placed atop discs of gel (~17 mm in diameter) before treatment with the CAP jet.

## 3. Results

### 3.1 CAP generation of H<sub>2</sub>O<sub>2</sub> in PBS

As previously reported, an increase in CAP exposure time results in a greater production of H<sub>2</sub>O<sub>2</sub> [28]. The CAP jet used and the time dependent generation of H<sub>2</sub>O<sub>2</sub> in PBS is shown in Figure 1. The KI calibration curve used to calculate concentration is shown in Figure 1 Supplementary Information.

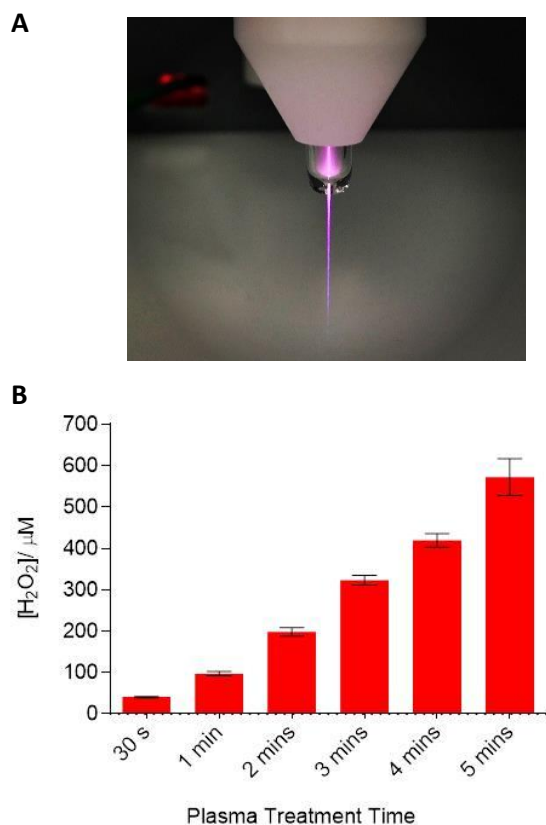


**Figure 1.** (A) CAP jet used in this study. (B) Generation of H<sub>2</sub>O<sub>2</sub> in PBS as a function of plasma treatment time. Means and standard deviations from three independent replicates are presented.

### 3.2 Temperature measurement of plasma jet

Measurement of the temperature of the plasma jet in contact with a *P. aeruginosa* biofilm reached a maximum temperature of 34 °C (Figure 2).

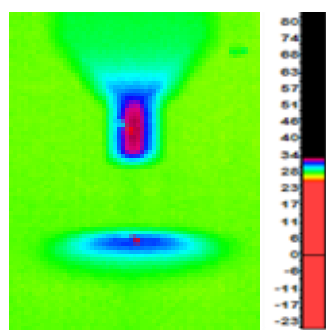


**Figure 2.** Temperature of plasma jet (top colour spot) showing a temperature gradient within the capillary tube and biofilm temperature at point of plasma contact (5 mm gap distance, image captured after 5 minutes, scale bar corresponds to temperature in °C).

### 3.3 CAP treatment of bacterial biofilms

The effect of biofilm maturity on the transmission of plasma-generated H<sub>2</sub>O<sub>2</sub> was first evaluated by calculating bacterial cell density of untreated biofilms at various time points, corresponding to biofilm incubation time. For comparative purposes, biofilms of Gram-positive MRSA 252 and Gram-negative *P. aeruginosa* PA01 were chosen as representative isolates commonly associated with chronic wound infection [37]. Further experiments were conducted evaluating the effect of CAP treatment on cell density as a function of biofilm maturity as shown in Figure 3. A scanning electron micrograph of a 24 hour biofilm is shown in the Supplementary Information (Figure 3) in order to highlight the density of the bacterial matrix.

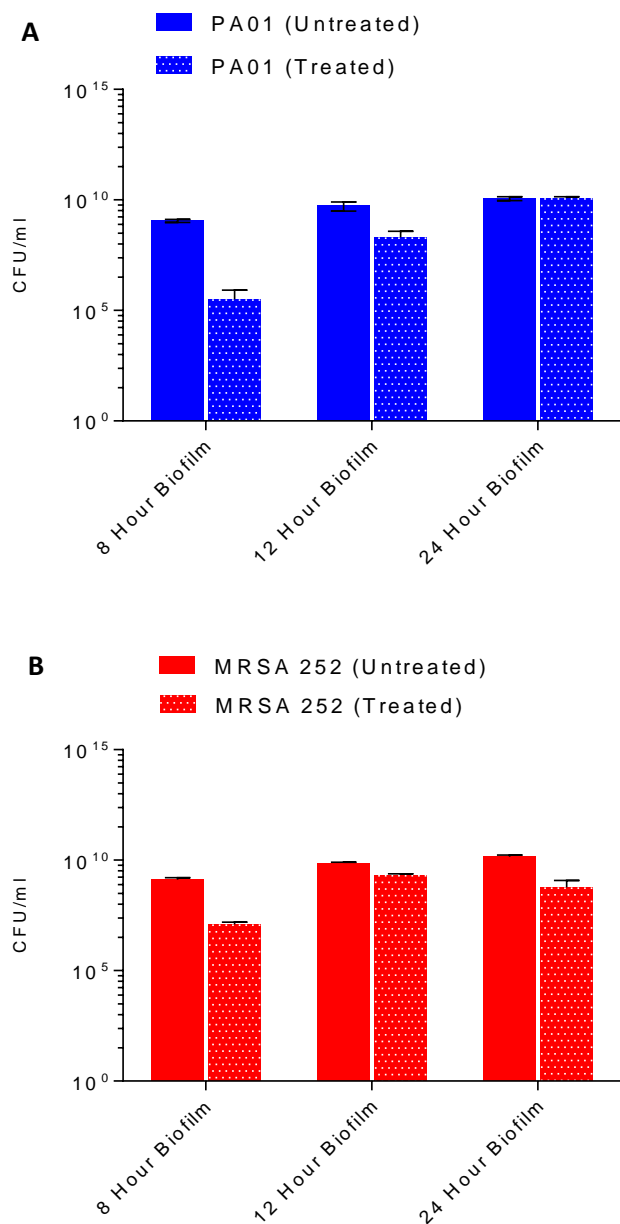


**Figure 3.** Effect of 5 minutes CAP treatment on cell density (CFU/ml) of *P. aeruginosa* PA01 (A) and MRSA 252 (B) biofilms at varying maturities relative to untreated control biofilms. Means and standard deviations from three biological replicates are presented.

Owing to the high bacterial cell densities in the biofilms used in this study, it is not unexpected that the application of CAP fails to reduce the density of the mature biofilms. Plasma treatment of 8 hour biofilms reduces the cell density but does not necessarily provide a clinically significant reduction in biomass with viable cell count remaining arguably high post treatment. Previous studies have focused on the recovery of biofilms post CAP treatment as a function of biofilm maturity [38]. Additional studies have been reported in which CAP

therapy is able to significantly reduce or even eliminate bacterial biofilms (albeit often when treating biofilms with a lower bioburden), however this study concerns the fate of CAP-generated RONS as opposed to their biological effect [39-40]. Therefore high density biofilms indicative of chronic infection were chosen as the cellular interface over which to monitor H<sub>2</sub>O<sub>2</sub> formation.

Prior to establishing the concentration of H<sub>2</sub>O<sub>2</sub> able to traverse the cellular interface, it was necessary to evaluate transmission across the polycarbonate membrane on which the biofilms were grown. Plasma treatment through the nanoporous membrane for 5 minutes resulted in a 33% reduction in H<sub>2</sub>O<sub>2</sub> concentration in the PBS below the membrane (relative to direct treatment of PBS), as shown in Figure 4. This was taken into account in subsequent experiments by the introduction of a transmission factor (TF) of 0.67 to account for the interference of the membrane.

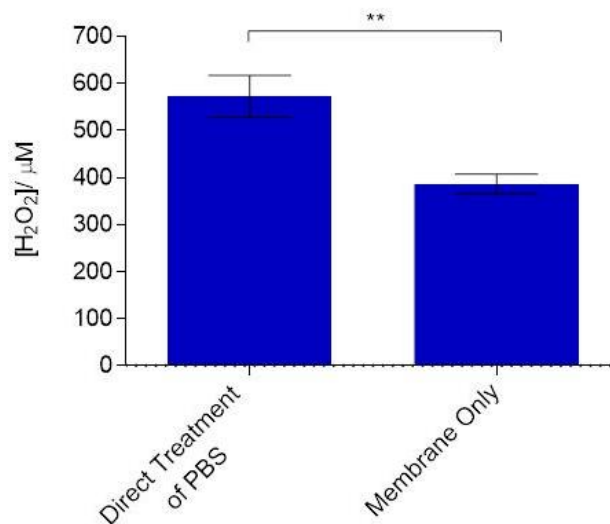


**Figure 4.** Effect of the polycarbonate membrane (a function of the experimental protocol) on the generation of H<sub>2</sub>O<sub>2</sub> in PBS after 5 minutes, showing a significant reduction in H<sub>2</sub>O<sub>2</sub> concentration. Means and standard deviations from three independent replicates are presented and have been analysed using an unpaired t test: \*\*  $p = 0.0029$ .

Considering the TF, the presence of AWF on the membranes (included as a pre-treatment prior to bacterial inoculation) was also investigated. Membranes were pre-treated with a conditioning layer of AWF and incubated at 37 °C for 8, 12 or 24 hours (in-keeping with subsequent biofilm growth conditions) to establish any interference from the conditioning layer over time. The concentration of H<sub>2</sub>O<sub>2</sub> generated in the PBS below the membrane impregnated with AWF was comparable to the membrane only (data shown in Figure 4), regardless of incubation time as summarised in Table 1.

Results illustrate no statistical significance with respect to  $\text{H}_2\text{O}_2$  concentration as a result of the inclusion of AWF or the incubation period. This suggests little measurable interference of the AWF on the transmission of  $\text{H}_2\text{O}_2$  across the interface.

**Table 1.** Concentration of  $\text{H}_2\text{O}_2$  generated across polycarbonate membranes inoculated with AWF following incubation for various time periods (taking into account the TF). Means and standard deviations from three biological replicates are presented and have been analysed using a one-way ANOVA with multiple comparisons.

Incubation Time/ hours	$[\text{H}_2\text{O}_2]/\text{TF}/\mu\text{M}$
8	$374.9 \pm 40.4$
12	$520.5 \pm 13.1$
24	$400.2 \pm 96.8$

However, Figure 5 shows the presence of bacterial biofilms (of all maturities) to have a significant effect on the transmission of  $\text{H}_2\text{O}_2$  relative to the membrane + AWF only. Biofilms grown for 8 hours, corresponding to approximately  $10^9$  CFU/ml, reduced the concentration of  $\text{H}_2\text{O}_2$  by approximately half, whereas biofilms approaching  $10^{10}$  CFU/ml almost entirely prevented the detection of  $\text{H}_2\text{O}_2$ . The results show a significant difference in  $\text{H}_2\text{O}_2$  concentration when comparing 8 hour biofilms of both MRSA and *P. aeruginosa* to the corresponding 12 and 24 hour biofilms, which may be as a direct result of the observed difference in bacterial cell death (seen in Figure 3) when comparing 8 hour biofilms to more mature biofilms. There is no significant difference observed between the 12 and 24 hour biofilms of either MRSA or *P. aeruginosa*; likewise, there is no difference in  $\text{H}_2\text{O}_2$  concentration between the bacterial species at each time point.

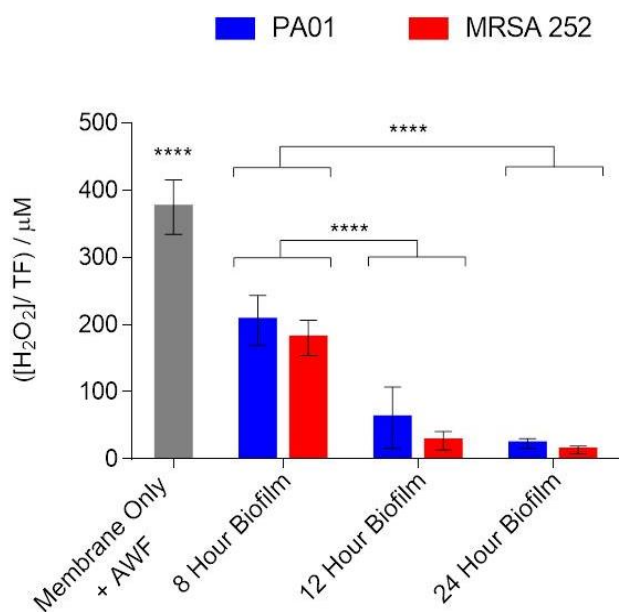


**Figure 5.** Effect of biofilm composition on the generation of  $\text{H}_2\text{O}_2$  in PBS below the interface as a function of biofilm maturity. Means and standard deviations from three biological replicates are presented and have been analysed using a two-way ANOVA with multiple comparisons: \*\*\*\*  $p < 0.0001$ .

In order to investigate time-dependent formation and/or diffusion of plasma-generated  $\text{H}_2\text{O}_2$ , PVA/ CMC hydrogels were used as a model system prior to commencing biofilm analysis. The gels were placed atop wells containing PBS and treated with the CAP jet for 5 minutes. The concentration of  $\text{H}_2\text{O}_2$  in the PBS was then determined immediately (0 hours incubation) and following incubation at  $32^\circ\text{C}$  (skin temperature) for 1 - 8 hours (Figure 5) [41]. In this case the incubation period facilitated the formation of  $\text{H}_2\text{O}_2$  in a time dependent manner over the course of 8 hours, reaching a maximum concentration within  $\sim 4$  hours.

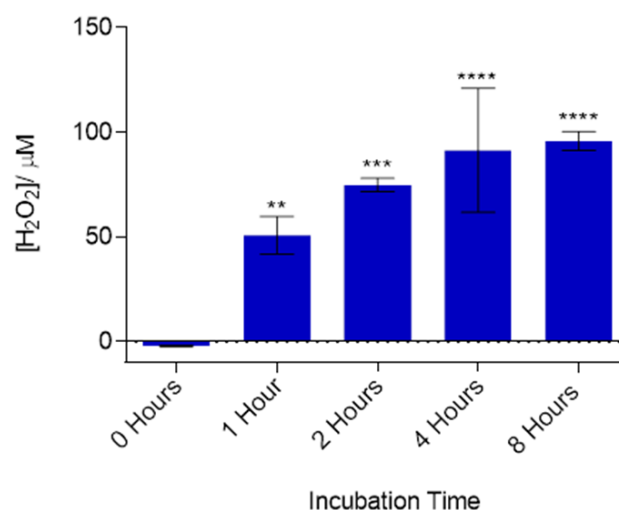


**Figure 6.** Effect of incubation time on  $\text{H}_2\text{O}_2$  concentration in PBS post CAP treatment of PVA/CMC hydrogels. Means and standard deviations from three independent replicates are presented and have been analysed using a one-way ANOVA with multiple comparisons: \*\*\*\*  $p < 0.0001$ , \*\*\*  $p < 0.001$ , \*\*  $p < 0.0001$ . Statistical significance is reported with respect to the concentration of  $\text{H}_2\text{O}_2$  detected immediately post exposure (0 hours).

However, this trend was not seen when subjecting 8 hour biofilms to the same incubation conditions. Conversely, the concentration of  $\text{H}_2\text{O}_2$  was lower for both MRSA and *P. aeruginosa* post incubation (Figure 7). Previous studies have indicated the role of catalase in protecting biofilms from the effects of hydrogen peroxide by catalysing its decomposition into oxygen and water [42-43]. Both *S. aureus* and *P.*

*aeruginosa* are catalase-positive, which could explain the results seen in Figure 7 using biofilms that had been incubated for 4 hours post CAP treatment. Further experimental studies will aim to address this point in the future.

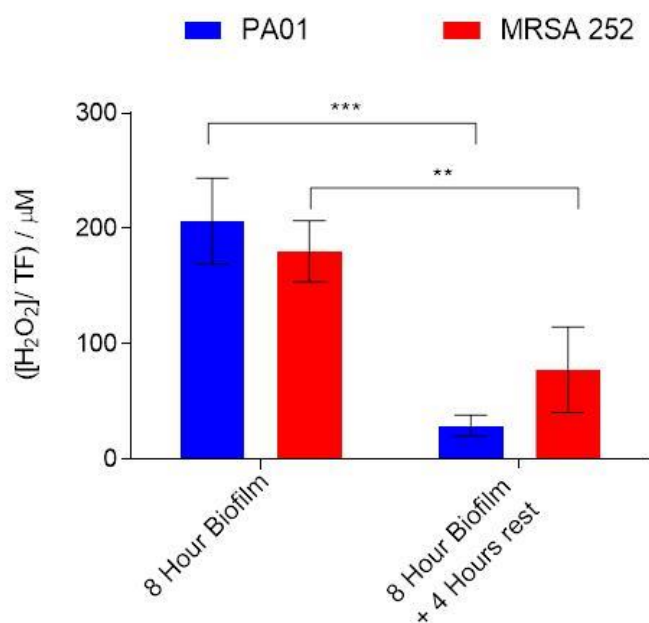


**Figure 7.** Effect of incubation time on H<sub>2</sub>O<sub>2</sub> concentration in PBS post CAP treatment of 8 hour biofilms. Means and standard deviations from three biological replicates are presented and have been analysed using a two-way ANOVA with multiple comparisons: \*\*\*  $p < 0.001$ , \*\*  $p < 0.0001$ .

### 3.4 Visualisation of H<sub>2</sub>O<sub>2</sub> formation

Qualitative assessment of H<sub>2</sub>O<sub>2</sub> formation (both immediately and over time) was undertaken using agarose gels containing KI. The hydrogel reservoir was able to indicate the formation and diffusion of CAP-generated H<sub>2</sub>O<sub>2</sub> through bacterial biofilms via a distinctive colour change upon the liberation of iodine. Biofilms were placed on the surface of the gels and subjected to CAP treatment. The gels were then imaged immediately following exposure, before being incubated for 4 hours at 32 °C, after which the biofilms were removed and the gels imaged once more. In agreement with previous quantitative data no colour change was observed within the gels during CAP treatment of 24 hour biofilms, whereas an immediate colour change was observed with 8 hour biofilms of both bacterial species (Supplementary Information Figures 5 and 6). However, when treating biofilms grown for 12 hours, MRSA biofilms facilitated a greater degree of iodine release within the agarose gels relative to *P. aeruginosa* biofilms grown for the same length of time. Figure 8 shows the colour change within the gels immediately post exposure (A and B) and after 4 hours incubation (C and D).

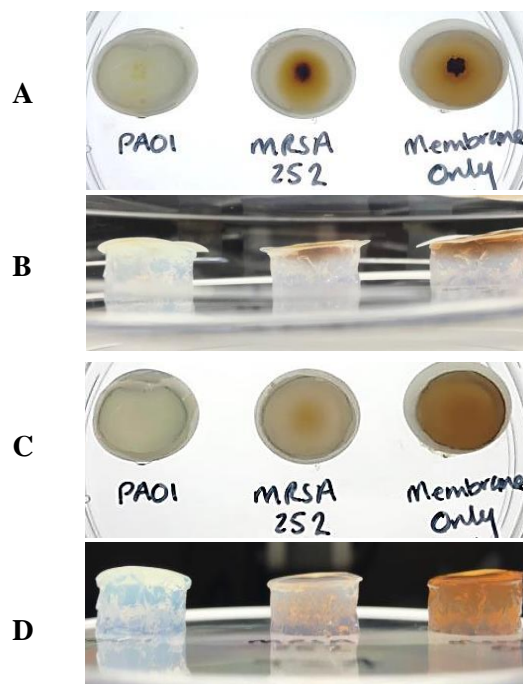


**Figure 8.** 12 hour biofilms of MRSA 252 and *P. aeruginosa* PA01 placed atop agarose gels containing KI and subject to CAP treatment imaged immediately post treatment (A, B) and after 4 hours incubation at 32 °C (C, D), compared to the uninoculated nanoporous membrane pre-treated with AWF.

This result contrasts with the quantitative data, which indicates very little H<sub>2</sub>O<sub>2</sub> generated across the 12 hour biofilms of both MRSA and *P. aeruginosa* into PBS (Figure 5). Indeed, within the range of the experimental error the concentration of H<sub>2</sub>O<sub>2</sub> below the biofilms is effectively equal for both species. However, in the case of biofilms placed atop a hydrogel surface there is a negligible colour change in the gel supporting the *P. aeruginosa* biofilms, whereas there is a clear colour change for the MRSA biofilms (albeit this change is small when compared to the ‘membrane only’ control). This discrepancy may be due to a number of factors; the delivery reservoir (PBS vs a gel matrix) is likely to affect the diffusion of reactive species and the uniformity of the biofilms may vary (they are matured by time as opposed to thickness and therefore there will undoubtedly be some variation). The behaviour of the biofilms when placed atop a liquid or solid interface may change and/or there may be a change in the H<sub>2</sub>O<sub>2</sub> catalysis under these conditions. Such considerations when designing experimental protocols for the analysis of CAP therapy should be carefully rationalised and investigated with respect to the intended application in order to more accurately predict and measure the possible outcomes.

### 3.5 Topical application of H<sub>2</sub>O<sub>2</sub>

Owing to the multitude of different processes occurring during CAP treatment which go beyond the direct operating parameters (to include gas mixing with atmospheric gases and mixing at the solution interface) it is challenging to provide a representative control for the analysis of plasma-generated species across biological interfaces [44]. Consequently, we have focused solely on H<sub>2</sub>O<sub>2</sub> transmission (as this is the major long-lived species generated by the jet described). H<sub>2</sub>O<sub>2</sub> at the same concentration as generated by the CAP jet in 5 minutes was topically applied to *P. aeruginosa* and MRSA biofilms determine equivalency between plasma-assisted penetration and topical therapy. Whilst it is difficult to compare the results directly, topically applied H<sub>2</sub>O<sub>2</sub> was unable to traverse biofilms of all maturities indicated by the absence of any quantifiable concentration of H<sub>2</sub>O<sub>2</sub> in the PBS reservoir below. This was confirmed immediately after the 5 minute exposure time and following a subsequent 4 hours incubation at 32 °C. This result suggests that plasma-generated H<sub>2</sub>O<sub>2</sub> (and possibly other CAP-generated RONS), are better able to penetrate bacterial biofilms than topical application of the same chemical species. Again, this is likely a result of the additional processes occurring, including continuous gas flow as a driving force into the biofilms, localised heating and/or synergistic effects from other plasma-generated RONS.

## 4. Discussion and Conclusions

The bioburden of the mature biofilms used in this study is arguably much higher than seen in some other studies. However, healthy skin is reportedly permanently colonised with 10<sup>3</sup> – 10<sup>4</sup> microorganisms per cm<sup>2</sup> skin (rising to 10<sup>6</sup> in moist areas), as part of a healthy skin microflora [45]. Therefore, dense biofilms with high microbial cell counts were used to represent the exponential proliferation of opportunistic pathogens associated with untreated chronic infection. In this study the use of CAP is intended as a therapeutic treatment as opposed to a preventative measure (whereby treatment may commence at lower cell densities than those often considered indicative of progressive infection).

In contrast to other studies, this work describes the effect of bacterial biofilms on the fate of plasma-generated products rather than any direct cellular effects of CAP therapy on the biofilms - an important consideration in the future clinical application of cold plasma. This investigation highlights the ability of plasma-generated reactive species to traverse live biofilms, remaining active despite interaction with the bacterial species present. This is observed up to cell densities of 10<sup>9</sup> CFU/ml, above which the concentration of longer lived species is significantly reduced when evaluated across the

interface of the biofilm. Determining the exact mechanism of cellular interaction with plasma-generated H<sub>2</sub>O<sub>2</sub> is ongoing. Owing to the complexity in determining the exact pathway of plasma-generated H<sub>2</sub>O<sub>2</sub> with respect to both the gas phase and the liquid interface, there are a number of considerations to take into account such as direct interaction of biofilm components (including catalase) with plasma-generated H<sub>2</sub>O<sub>2</sub>, alongside the transport and any subsequent reactions with additional plasma-generated RONS [46-47]. Nonetheless, the ability of high density bacterial biofilms to influence the transmission of such species may have implications for the application of CAP therapy in the treatment of chronic infection, whereby high bacterial loads may be readily encountered. In the context of deep-seated infections, the ability to deliver RONS directly into the infected tissues may vary with different device designs or may in fact be a ubiquitous challenge associated with CAP therapy. This should be established with the intention of improving RONS delivery and penetration in order to successfully apply this technology to highly contaminated wounds. Alongside ensuring the efficacy of CAP therapy via adequate penetration and delivery of plasma-generated reactive species, the effects of such species on other cellular entities cannot be underestimated. Ultimately, for the successful therapeutic treatment of infection, a balance must be established between efficacious elimination of pathogenic organisms and implementation of adequate controls for the protection of the surrounding host tissue.

Further research will focus on establishing the effect of catalase on the lifetime and bioavailability of plasma-generated H<sub>2</sub>O<sub>2</sub>, the effect of CAP-induced bacterial cell death on the transmission of H<sub>2</sub>O<sub>2</sub> and any protective effects offered by bacterial biofilms with respect to surrounding host tissues. Additional research will also aim to investigate the formation and transmission of other reactive species such as O<sub>2</sub><sup>·-</sup>, ·OH, ·HO<sub>2</sub>, to determine additional transportation mechanisms of plasma-generated RONS with respect to the material interface (biotic or abiotic).

## Acknowledgements

The authors would like to thank the EPSRC for grant EP/R003556/1. B Patenall would like to thank James Tudor and Mr and Mrs Watson for additional funding. G Williams would also like to thank Public Health England.

## References

- [1] 2017 Innovative Medicines Initiative, ND4BB New Drugs for Bad Bugs
- [2] 2015 CDC National Action Plan for the Combating Antibiotic-Resistant Bacteria



- [3] 2015 World Health Organisation, Global Action Plan on Antimicrobial Resistance
- [4] O'Neill J 2016 Tackling Drug-Resistant Infections Globally: Final Report and Recommendations.
- [5] Jamal M, Ahmad W, Andleeb S, Jalil F, Imran M, Nawaz M A, Hussain T, Ali M, Rafiq M and Kamil M A 2018 Bacterial biofilm and associated infections *Journal of the Chinese Medical Association* **81** 7-11
- [6] Herman-Bausier P and Dufrene Y F 2018 Force matters in hospital-acquired infections *Science* **359** 1464-5
- [7] Flanagan M E, Welsh C A, Kiess C, Hoke S and Doebbeling B N 2011 A national collaborative for reducing health care-associated infections: current initiatives, challenges, and opportunities *American Journal of Infection Control* **39** 685-9
- [8] Phillips C J, Humphreys I, Fletcher J, Harding K, Chamberlain G and Macey S 2016 Estimating the costs associated with the management of patients with chronic wounds using linked routine data *International Wound Journal* **13** 1193-7
- [9] Gottrup F 2004 A specialized wound-healing center concept: importance of a multidisciplinary department structure and surgical treatment facilities in the treatment of chronic wounds *American Journal of Surgery* **187** 38S-43S
- [10] 2009 The Wound Healing Society, Chronic Wound Care Guidelines.
- [11] Jarbrink K, Ni G, Sonnergren H, Schmidtchen A, Pang C, Bajpai R and Car J 2017 The humanistic and economic burden of chronic wounds: a protocol for a systematic review *Systematic Reviews* **6** 7
- [12] Omar A, Wright J B, Schultz G, Burrell R and Nadworny P 2017 Microbial Biofilms and Chronic Wounds *Microorganisms* **5** 15
- [13] Modic M, McLeod N P, Sutton J M and Walsh J L 2017 Cold atmospheric pressure plasma elimination of clinically important single- and mixed-species biofilms *International Journal of Antimicrobial Agents* **49** 375-8
- [14] Mai-Prochnow A, Clauson M, Hong J M and Murphy A B 2016 Gram positive and Gram negative bacteria differ in their sensitivity to cold plasma *Scientific Reports* **6** 11
- [15] Flynn P B, Higginbotham S, Alshraiedeh N H, Gorman S P, Graham W G and Gilmore B F 2015 Bactericidal efficacy of atmospheric pressure non-thermal plasma (APNTP) against the ESKAPE pathogens *International Journal of Antimicrobial Agents* **46** 101-7
- [16] Laroussi M, Lu X and Keidar M 2017 Perspective: The physics, diagnostics, and applications of atmospheric pressure low temperature plasma sources used in plasma medicine *Journal of Applied Physics* **122**
- [17] Lu X, Naidis G V, Laroussi M, Reuter S, Graves D B and Ostrikov K 2016 Reactive species in non-equilibrium atmospheric-pressure plasmas: Generation, transport, and biological effects *Physics Reports-Review Section of Physics Letters* **630** 1-84
- [18] O'Connor N, Cahill O, Daniels S, Galvin S and Humphreys H 2014 Cold atmospheric pressure plasma and decontamination. Can it contribute to preventing hospital-acquired infections? *Journal of Hospital Infection* **88** 59-65
- [19] Mai-Prochnow A, Murphy A B, McLean K M, Kong M G and Ostrikov K 2014 Atmospheric pressure plasmas: Infection control and bacterial responses *International Journal of Antimicrobial Agents* **43** 508-17
- [20] Gilmore B F, Flynn P B, O'Brien S, Hickok N, Freeman T and Bourke P 2018 Cold Plasmas for Biofilm Control: Opportunities and Challenges *Trends in Biotechnology* **36** 627-38
- [21] Flynn P B and Gilmore B F 2018 Understanding plasma biofilm interactions for controlling infection and virulence *Journal of Physics D: Applied Physics* **51**
- [22] Haertel B, von Woedtke T, Weltmann K D and Lindequist U 2014 Non-Thermal Atmospheric-Pressure Plasma Possible Application in Wound Healing *Biomolecules & Therapeutics* **22** 477-90
- [23] Rödder K, Gandhirajan R, von Woedtke T and Bekeschus S 2018 Where Do Ros Go? Oxidation Cascades In Melanoma Exposed To Cold Physical Plasma *Clinical Plasma Medicine* p29
- [24] Boehm D, Heslin C, Cullen P J and Bourke P 2016 Cytotoxic and mutagenic potential of solutions exposed to cold atmospheric plasma *Scientific Reports* **6**
- [25] Oh J S, Strudwick X, Short R D, Ogawa K, Hatta A, Furuta H, Gaur N, Hong S H, Cowin A J, Fukuhara H, Inoue K, Ito M, Charles C, Boswell R W, Bradley J W, Graves D B and Szili E J 2016 How plasma induced oxidation, oxygenation, and de-oxygenation influences viability of skin cells *Applied Physics Letters* **109**
- [26] Szili E J, Hong S H, Oh J S, Gaur N and Short R D 2018 Tracking the Penetration of Plasma Reactive Species in Tissue Models *Trends in Biotechnology* **36** 594-602
- [27] Marshall S E, Jenkins A T A, Al-Bataineh S A, Short R D, Hong S H, Thet N T, Oh J S, Bradley J W and Szili E J 2013 Studying the cytolytic activity of gas

- plasma with self-signalling phospholipid vesicles dispersed within a gelatin matrix *Journal of Physics D-Applied Physics* **46**
- [28] Oh J S, Szili E J, Gaur N, Hong S H, Furuta H, Kurita H, Mizuno A, Hatta A and Short R D 2016 How to assess the plasma delivery of RONS into tissue fluid and tissue *Journal of Physics D-Applied Physics* **49**
- [29] Szili E J, Bradley J W and Short R D 2014 A 'tissue model' to study the plasma delivery of reactive oxygen species *Journal of Physics D-Applied Physics* **47**
- [30] Szili E J, Gaur N, Hong S H, Kurita H, Oh J S, Ito M, Mizuno A, Hatta A, Cowin A J, Graves D B and Short R D 2017 The assessment of cold atmospheric plasma treatment of DNA in synthetic models of tissue fluid, tissue and cells *Journal of Physics D-Applied Physics* **50**
- [31] Chen C, Liu D X, Liu Z C, Yang A J, Chen H L, Shama G and Kong M G 2014 A Model of Plasma-Biofilm and Plasma-Tissue Interactions at Ambient Pressure *Plasma Chemistry and Plasma Processing* **34** 403-41
- [32] Xiong Z, Du T, Lu X, Cao Y and Pan Y 2011 How deep can plasma penetrate into a biofilm? *Applied Physics Letters* **98**
- [33] Pei X, Lu X, Liu J, Liu D, Yang Y, Ostrikov K, Chu P K and Pan Y 2012 Inactivation of a 25.5µm *Enterococcus faecalis* biofilm by a room-temperature, battery-operated, handheld air plasma jet *Journal of Physics D: Applied Physics* **45**
- [34] Gorbanev Y, O'Connell D and Chechik V 2016 Non-Thermal Plasma in Contact with Water: The Origin of Species *Chemistry: A European Journal* **22** 3496.
- [35] Junglee S, Urban L, Sallanon H and Lopez-Lauri F 2014 Optimized Assay for Hydrogen Peroxide Determination in Plant Tissue Using Potassium Iodide *American Journal of Analytical Chemistry* **05** 730
- [36] Thet N T, Wallace L, Wibaux A, Boote N and Jenkins A T A 2018 Development of a mixed-species biofilm model and its virulence implications in device related infections *Journal of Biomedical Materials Research Part B Applied Biomaterials* **107** 129-37
- [37] Bowler P G, Duerden B I and Armstrong D G 2001 Wound microbiology and associated approaches to wound management *Clinical Microbiology Reviews* **14** 244
- [38] Patenall B L, Hathaway, H., Sedgwick, A.C., Thet, N.T., Williams, G.T., Young, A.E., Allinson, S.L., Short, R.D. and Jenkins, A.T.A. 2018 Limiting *Pseudomonas aeruginosa* Biofilm Formation Using Cold Atmospheric Pressure Plasma *Plasma Medicine* **8** 269-277
- [39] Ziuzina D, Boehm D, Patil S, Cullen P J and Bourke P 2015 Cold Plasma Inactivation of Bacterial Biofilms and Reduction of Quorum Sensing Regulated Virulence Factors *PLoS ONE* **10**
- [40] Alkawareek M Y, Algwari Q T, Laverty G, Gorman S P, Graham W G, O'Connell D and Gilmore B F 2012 Eradication of *Pseudomonas aeruginosa* Biofilms by Atmospheric Pressure Non-Thermal Plasma *PLOS ONE* **7**
- [41] Fierheller M and Sibbald G 2010 A Clinical Investigation into the Relationship between Increased Periwound Skin Temperature and Local Wound Infection in Patients with Chronic Leg Ulcers *Advances in Skin & Wound Care* **23** 369-78
- [42] Stewart S P, Roe F, Rayner J, Elkins J G, Lewandowski Z, Ochsner U A and Hassett D J 2000 Effect of Catalase on Hydrogen Peroxide Penetration into *Pseudomonas aeruginosa* Biofilms *Applied and Environmental Microbiology* **66** 836 – 838
- [43] Ochieng' Olwal C, Oyieng' Ang'ienda P and Otieno Ochiel D 2019 Alternative sigma factor B ( $\sigma$ B) and catalase enzyme contribute to *Staphylococcus epidermidis* biofilm's tolerance against physico-chemical disinfection *Scientific Reports* **9**
- [44] Girard F, Peret M, Dumont et al., 2018 Correlations between gaseous and liquid phase chemistries induced by cold atmospheric plasmas in a physiological buffer, *Physical Chemistry Chemical Physics*, **20**, 9198-9210
- [45] Greene J N 1996 The microbiology of colonization, including techniques for assessing and measuring colonization *Infection Control and Hospital Epidemiology* **17** 114-8
- [46] Bruggeman P and Schram D C 2010 On OH production in water containing atmospheric pressure plasmas *Plasma Sources Science and Technology* **19**
- [47] Liu J, He B, Chen Q, Li J, Xiong Q, Yue G, Zhang X, Yang S, Liu H and Liu QH 2016 Direct synthesis of hydrogen peroxide from plasma-water interactions *Scientific Reports* **5**